Theor. Appl. Climatol. (2008) 94: 125–137
DOI 10.1007/s00704-007-0358-5
Printed in The Netherlands

Theoretical and Applied Climatology

[1] Department of Physical Oceanography, Institute of Oceanography, University of São Paulo, São Paulo, SP, Brazil
[2] Department of Atmospheric Sciences, Institute of Astronomy, Geophysics and Atmospheric Sciences, University of São Paulo, São Paulo, SP, Brazil

The role of the South Indian and Pacific oceans in South American monsoon variability

A. R. de M. Drumond[1], **T. Ambrizzi**[2]

With 7 Figures

Received 30 October 2006; Accepted 5 September 2007; Published online 20 February 2008

Summary

This work has investigated the impact of three different low-frequency sea surface temperature (SST) variability modes located in the Indian and the Pacific Oceans on the interannual variability of the South American Monsoon System (SAMS) using observed and numerical data. Rotated Empirical Orthogonal Function (REOF) analysis and numerical simulations with a General Circulation Model (GCM) were used. One of the three SST variability modes is located close to southeastern Africa. According to the composites, warmer waters over this region are associated with enhanced austral summer precipitation over the sub-tropics. The GCM is able to reproduce this anomalous precipitation pattern, simulating a wave train emanating from the Indian Ocean towards South America (SA). A second SST variability mode was located in the western Pacific Ocean. REOF analysis indicates that warmer waters are associated with drought conditions over the South Atlantic Convergence Zone (SACZ) and enhanced precipitation over the sub-tropics. The GCM indicates that the warmer waters over Indonesia generate drought conditions over tropical SA through a Pacific South America-like (PSA) wave pattern emanating from the western Pacific. Finally, the third SST variability mode is located over the southwestern South Pacific. The composites indicate that warmer waters are associated with enhanced precipitation over the SACZ and drought conditions over the sub-tropics. There is a PSA-like wave train emanating from Indonesia towards SA, and another crossing the Southern Hemisphere in the extra-tropics, probably associated with transient activity. The GCM is able to reproduce the anomalous precipitation pattern, although it is weaker than observed. The PSA-like pattern is simulated, but the model fails in reproducing the extra-tropical wave activity.

Correspondence: Anita Rodrigues de Moraes Drumond, Department of Physical Oceanography, Institute of Oceanography, University of São Paulo, Praça do Oceanográfico 191, São Paulo, SP 05508-120, Brazil, e-mail: adrumond@io.usp.br

1. Introduction

During the austral summer the highest values of South American precipitation occur over northern Brazil with an extension of secondary maxima emanating from this region towards southeast Brazil, as can be observed in fig. 2 of Grimm et al. (2005). According to these authors and references therein, the seasonal cycle of precipitation over most of South America presents maximum values during the austral summer season and minimum in the winter, characterizing therefore, the South American Monsoon System (SAMS) (Zhou and Lau 2001).

Grimm et al. (2005) describe the general features of the SAMS configuration. In the austral summer a thermal low-pressure system is ob-

served over the Chaco region, in central South America, increasing the southwest-northeast inter-hemispheric pressure gradient between the South American low and northwestern Sahara. The moist northeasterly trade winds then strengthen and penetrate South America. Over the continent, this flow becomes northwesterly, is channelled southward by the Andes, and turns clockwise around the Chaco low. Low-level wind and moisture convergence associated with the interaction of the continental low with the South Atlantic High and the northeasterly trade winds result in enhanced precipitation in the Amazon, and central and southeastern Brazil (Lenters and Cook 1995). The southeastward extension of cloudiness and precipitation towards the Atlantic Ocean is referred to as the South Atlantic Convergence Zone (SACZ) (Kodama 1992; Figueroa et al. 1995; Liebmann et al. 1999).

Another important system for the South American climate is the low level Jet (LLJ), which modulates precipitation over southern Brazil and the La Plata Basin. The LLJ is observed over a region close to the eastern Andes and contributes to the meridional moisture transport from the Amazon to the sub-tropics (Marengo et al. 2002, 2004, and references therein).

The existence of a precipitation dipole pattern over South America, identified through statistical analysis at the intraseasonal scale, was first suggested by Casarin and Kousky (1986). A similar structure for this dipole pattern can also be observed at the interannual or even at lower frequency variability scales (Robertson and Mechoso 2000). Herdies et al. (2002) verified two main summer circulation patterns over the continent: one associated with the occurrence of SACZ events and another with their absence. According to the authors, during SACZ events there is an intense LLJ carrying moisture from the Atlantic Ocean and Amazon to the sub-tropics, associated with moisture flux convergence and precipitation over the Amazon Basin and southeastern Brazil. The weakening of moisture transport to the La Plata Basin causes a reduction in precipitation over northern Argentina, Paraguay, southern Bolivia and northern Chile. On the other hand, when SACZ events are absent, the LLJ is displaced westward and moisture transport over the SACZ region is interrupted, weakening moisture flux convergence over southeastern Brazil and restricting moisture transport, mainly over the La Plata Basin.

The modulation, not only of the SACZ events, but also of the South American climate, can be influenced by the sea surface temperature (SST). The influence of El Niño-southern Oscillation (ENSO) events over the South American precipitation is now well-known (Grimm et al. 1998, and others). In general, during El Niño (EN) events precipitation is enhanced over southeastern South America due to the intensification of the Sub-tropical Jet and to a persistent atmospheric blocking (e.g., Ropelewski and Halpert 1987; Diaz et al. 1998). On the other hand, droughts occur over northeastern Brazil due to the displacement of the Walker Cell (e.g., Ropelewski and Halpert 1987; Ambrizzi et al. 2004).

In the South Pacific, Barros and Silvestri (2002) verified that the sub-tropical south-central Pacific (SSCP) and the central-east equatorial Pacific have an effect on the interannual variability of precipitation observed over southeastern South America during the austral spring. Moreover, they found that inter-El Niño precipitation variability over this region is modulated mainly by the SSCP. Therefore, the occurrence of positive (negative) anomalies of precipitation over southeastern South America is associated with negative (positive) SST anomalies over SSCP.

Recent studies have found that the Indian Ocean may play an important role in the climate of South American. Saji et al. (2005) verified a relationship between the Indian Ocean Dipole and air temperature over sub-tropical South America in the austral spring. The link between these two regions occurs through a Rossby wave train propagating from eastern Indian towards Sub-tropical Pacific and Atlantic via Sub-tropical and Sub-polar Jet streams which may act as wave guides (e.g., Hoskins and Ambrizzi 1993).

We will here demonstrate the importance of three different low-frequency SST variability modes located in the Indian and the Pacific Oceans in the interannual variability of the SAMS. Section 2 presents the data, methodology and a brief description of the numerical model used. Section 3 presents the statistical and the numerical analyses, and Sect. 4 summarizes the main results found.

2. Data and methods

The $2^\circ \times 2^\circ$ Smith et al. (1996) SST data set was used in this study. The $2.5^\circ \times 2.5^\circ$ monthly precipitation anomalies of Chen et al. (2002) were used to prepare the composites, as well as the $2.5^\circ \times 2.5^\circ$ National Centre for Atmospheric Research (NCAR) Reanalysis data set (Kalnay et al. 1996). The Smith and the Reanalysis data sets are available on the CDC National Oceanic and Atmospheric Administration – Cooperative Institute for Research in Environmental Sciences (NOAA – CIRES) web site. The climatology was defined for the period from 1950 to 2001.

Rotated Empirical Orthogonal Function (REOF) analysis was applied to the normalized summer (December, January and February, DJF) SST anomalies observed during the period 1950–2001 in the South Pacific + Equatorial Pacific (SEP) (40° S–18° N; 120–286°) and in the Indian (IN) (40° S–32° N; 20–116°) Oceans. For each analysis, the modes obtained via EOF were rotated using normalized Varimax. Extreme events were selected by applying the one standard deviation threshold over its normalized principal component (PC) time series, which were then studied through composites. Three modes were selected for study due to their importance to the SAMS.

The atmospheric General Circulation Model (GCM) used is the NCAR Community Climate Model 3.6 (CCM3.6). It is a spectral global model and T42L18 resolution was used for this study. Some detailed descriptions of the model can be found in Kiehl et al. (1998) and Hurrell et al. (1998).

The model was forced with the positive signal of selected SST modes, considered as SST anomalies, through an ensemble technique with five simulations using different initial conditions (IC). These ICs were extracted from a 10 year-long integration forced by the climatological cycle of SST.

The forcing for each experiment considers the correlation between the temporal series of the PC related to the mode and the temporal series of the observed SST anomalies as SST anomalies. This "anomalous field" was multiplied by the factor 3 to amplify its values. The simulations were run from September/year 0 to March/year 1 and the SST anomalies were kept constant during the integration, while the monthly SST climatology varied. This method is similar to that presented by Haarsma et al. (2003) and Robertson et al. (2003).

In this way, the anomaly calculated for the numerical experiments was defined as the difference between each ensemble mean and the average of the 10 year-long control integration.

A two-sided Student's *t*-test was applied to assess the statistical significance of the observational and numerical results. For the numerical results, the test was applied to each experiment according to Eq. (1)

$$t = \frac{X_M - R}{\{S_M^2/N\}^{1/2}} \quad (1)$$

where X_M and S_M^2 are, respectively, the 5-member ensemble mean and the variance of the ensemble members, R is the 10-year control integration mean, and N is the size of the ensemble. Due to the small number of ensemble members, the *t*-test was computed with 90% confidence and $N-1$ degrees of freedom. Only the statistically significant results are discussed here.

3. Results

3.1 The impact of South Indian SST anomalies on South American precipitation during the austral summer

Before discussing the results, it is important to note that the grey colour in Figs. 1, 3 and 5a indicates regions where the correlation is statistically significant at the 95% level according to the *t*-test. In the other figures, the grey and the vector show statistically significant anomalies at the 90% level.

The second SST variability mode found for the Indian Ocean (IN) region explains 12% of the total variance and is located around 25° S, 80° E (Fig. 1a). According to the composites, warmer waters over this region are associated with enhanced austral summer precipitation over subtropical South America and drought conditions over the tropics (Fig. 1b). The vertically integrated anomalous moisture flux presents an anomalous northerly flux and moisture convergence over the La Plata Basin (Fig. 1c). At high levels, the atmospheric circulation composite presents an anomalous wave pattern propagating through South Indian and bifurcating around western Australia, where part of the train crosses the con-

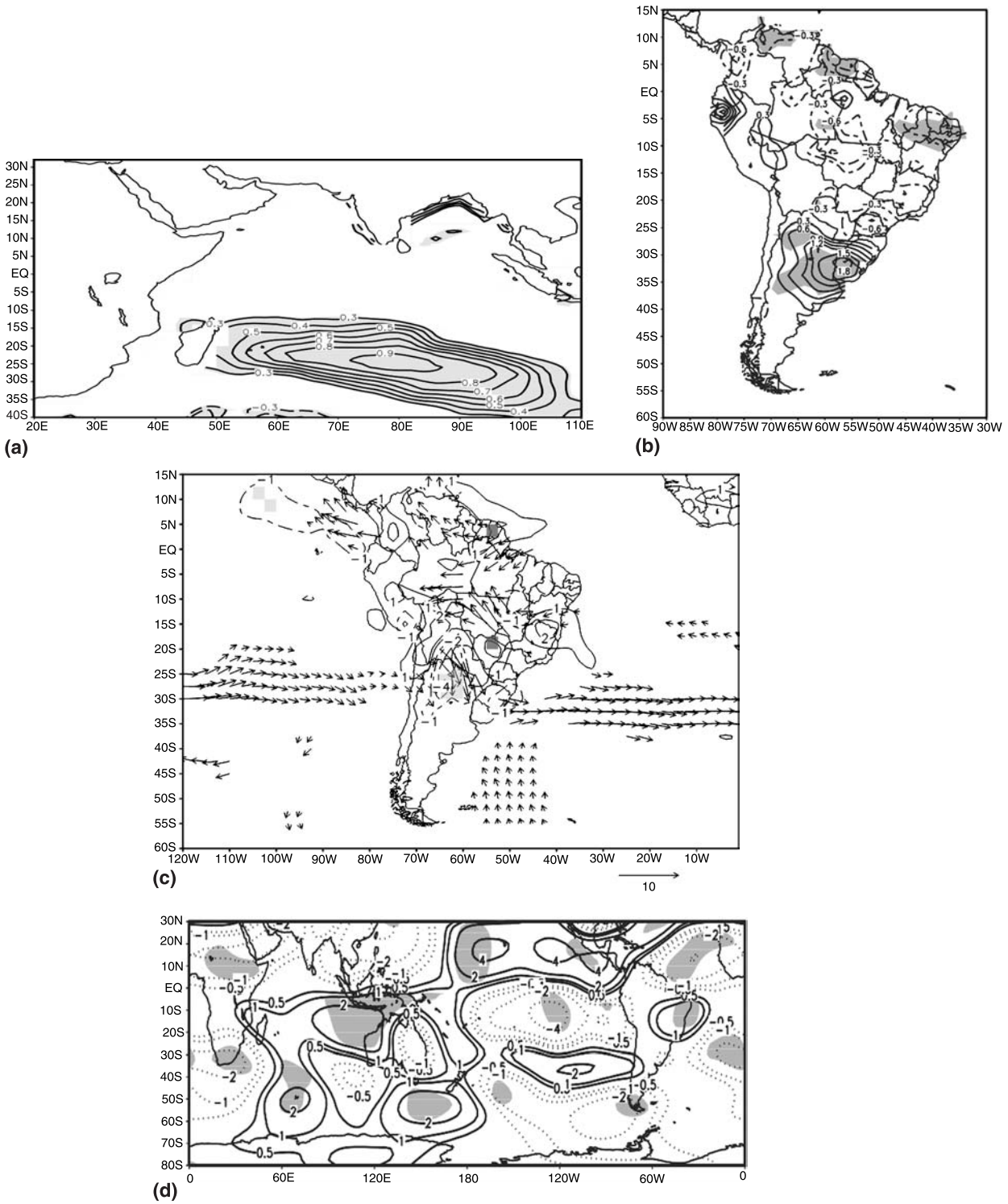

Fig. 1. (**a**) Pattern of the second rotated SST variability mode observed in the southern Indian Ocean during the austral summer expressed as correlation coefficients. Only isolines with absolute values higher than 0.3 are presented, with the interval of 0.1; (**b**) composite of DJF precipitation anomalies (mm day^{-1}) for the warm extreme events of the second rotated IN mode. The interval between the isolines is 0.3 mm day^{-1}; (**c**) the same as **b**, but for the DJF vertically integrated moisture flux ($\times 10^2$ g cm^{-1} s^{-1}) (vector) and the divergence associated (mm day^{-1}) (shaded and contour lines, respectively). For divergence, the absolute values of the isolines are 1; 2; 4 mm day^{-1}; (**d**) the same as **b**, but for the DJF 200 hPa anomalous zonally asymmetric component of stream function ($\times 10^6$ m^2 s^{-1}). The absolute values of the isolines are 0.5; 1; 2; 4; 6×10^6 m^2 s^{-1}. Negative values are shown with dash contours

tinent in a meridional trajectory and the other retains its arch-like propagation through the extra-tropics towards the eastern Pacific (Fig. 1d). In this region, waves propagate towards the tropics while another wave train continues its propagation through the extra-tropics. This wave

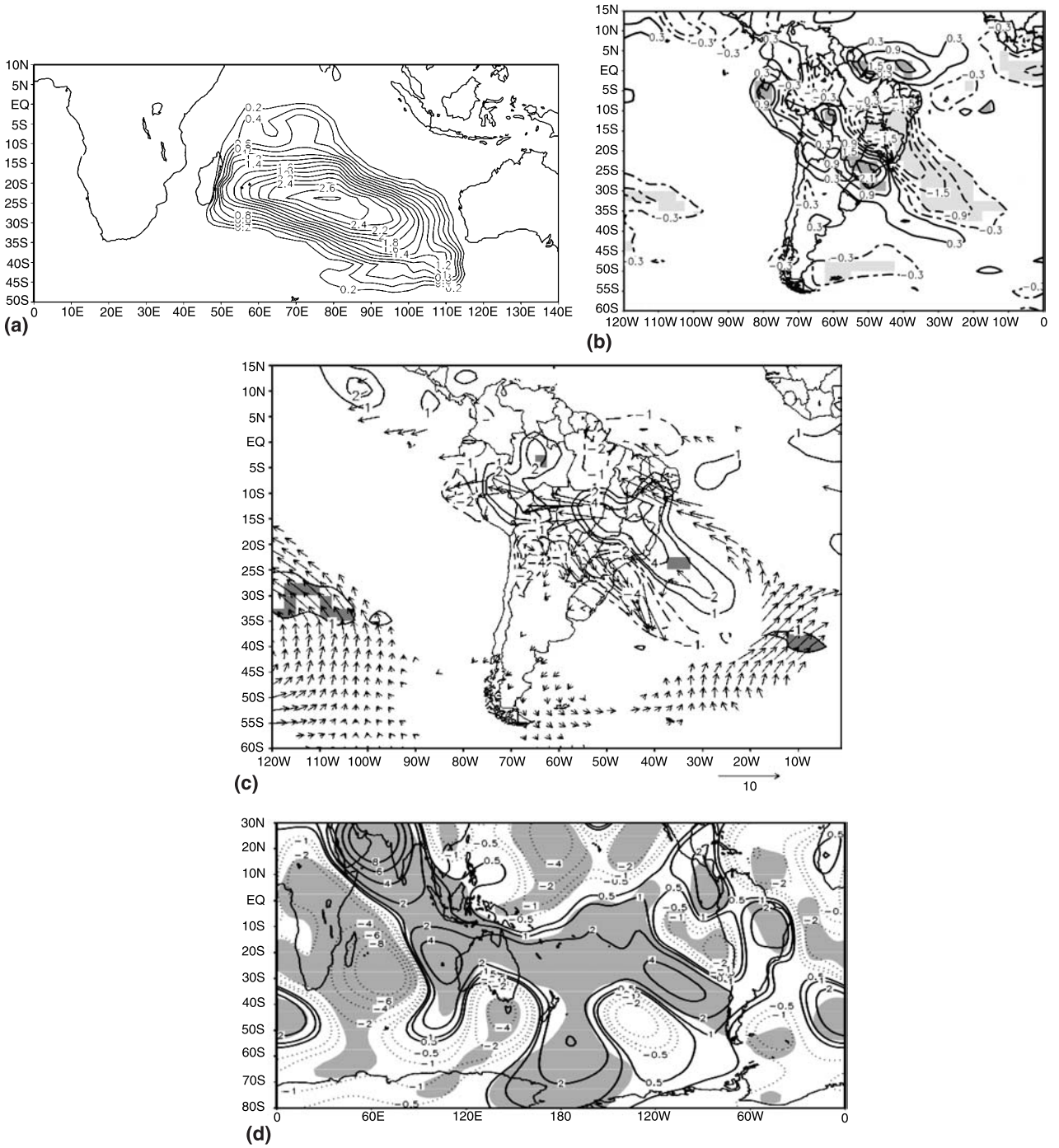

Fig. 2. (**a**) SST anomalies (°C) used in the numerical experiment forced with the warm phase of the second rotated IN mode. The interval between isolines is 0.2 °C; (**b**) DJF precipitation anomalies (mm day^{-1}) simulated in the experiment forced by the SST anomalies given in the Fig. 2a. Only absolute values higher than 0.3 mm day^{-1} are shown and the interval between the isolines is 0.6 mm day^{-1}; (**c**) the same as **b**, but for the DJF vertically integrated moisture flux ($\times 10^2$ g cm^{-1} s^{-1}) (vector) and the divergence associated (mm day^{-1}) (shaded and contour lines); (**d**) the same as **b**, but for the DJF 200 hPa anomalous zonally asymmetric component of stream function ($\times 10^6$ m^2 s^{-1}). The absolute values of the isolines in **c** and **d** are the same used in the Fig. 1c and d, respectively

propagation pattern suggests that the Sub-polar Jet may be acting as a wave guide. In fact, Hoskins and Ambrizzi (1993) verified, through numerical experiments, that the Southern Hemisphere Sub-polar Jet, located around 50° S over the Indian Ocean, can act as a wave guide. They also observed the bifurcation of the associated wave activity in eastern Australia, where the guide weakens. Part of the activity propagates over Australia and the remainder travels in an arching pattern towards the eastern Pacific and South Atlantic. This pattern was also verified by Berbery et al. (1992) on an intraseasonal time scale.

The model was forced with the SST anomalies shown in Fig. 2a. The precipitation and atmospheric circulation patterns simulated are presented in Fig. 2b–d. The drought conditions over central-eastern Brazil and enhanced precipitation over southern Brazil (Fig. 2b) are in good agreement with the observations (Fig. 1b). The simulated vertically integrated anomalous moisture flux (Fig. 2c) also agrees with the composite (Fig. 1c), though the model displaces slightly the maximum anomalous convergence in the sub-tropics to the east. At high levels, the simulated stream function anomalies (Fig. 2d) are similar to the anomalous patterns found in the composite (Fig. 1d).

From the comparison of the statistical and numerical results one can see that the warm phase of the Indian Ocean SST variability mode may have some impact on anomalous precipitation patterns over South America (Fig. 1b). The link between these two regions begins with perturbation generated in the Indian Ocean, which trigger a wave train that propagates inside of Sub-polar Jet waveguide towards the South American continent. As previously discussed, Saji et al. (2005) also suggested a similar teleconnection pattern, where the Indian Ocean Dipole influences air temperature in sub-tropical Australia, Africa and South America through Rossby wave train propagation from eastern Indian towards the sub-tropical Pacific and Atlantic through the sub-tropical and sub-polar Jets waveguides.

3.2 The impact of western Pacific SST anomalies on South American precipitation during the austral summer

The second mode obtained in the SEP region (explaining 12.4% of the total variance) consists of a region extending from the sub-tropical southwestern Pacific towards Indonesia, where the maximum loading is located (Fig. 3a). REOF analysis indicates that warmer waters over this region are associated with drought conditions over the SACZ and enhanced precipitation over sub-tropical South America (Fig. 3b).

The vertically integrated anomalous moisture flux presents an anomalous easterly flux over southeastern and central Brazil (Fig. 3c), probably associated with the inhibition of the occurrence of SACZ events (Nogués-Paegle and Mo 1997). One of the mechanisms associated with the manifestation of the SACZ is the low-level moisture transport from the Amazon to southeastern Brazil (Kodama 1992). Consequently, large anomalous moisture flux divergence occurred over central Brazil and the southeastern Brazilian coast, whilst anomalous westerly moisture flux and convergence was observed over southern Brazil (Fig. 3c).

At upper levels, atmospheric circulation composites show an anomalous wave train emanating from the western Pacific towards South America through the sub-tropics (Fig. 3d). Anticyclonic anomalous circulation is seen over western South America with its domain extending towards southern Brazil.

The PC time series (not shown) it revealed that the 2000/2001 austral summer experienced the highest magnitude of extreme events. During this season, a severe drought was observed over eastern Brazil which trigged an energy crisis in the country. A complete discussion of this case study can be found in Drumond and Ambrizzi (2005) who also indicated, through numerical simulations, that the combined influence of the SST anomalies observed in the South Pacific and Equatorial Pacific in that year were responsible for the precipitation anomaly patterns obtained. It is interesting to note that the anomalous precipitation pattern observed during this event is quite similar to the composite presented in Fig. 3b.

The model was forced with the SST anomalies shown in Fig. 4a. In agreement with the composite map (Fig. 3b), the simulated precipitation anomalies show positive values in sub-tropical South America and a well configured drought over eastern Brazil (Fig. 4b). The simulated vertically integrated anomalous moisture flux (Fig. 4c)

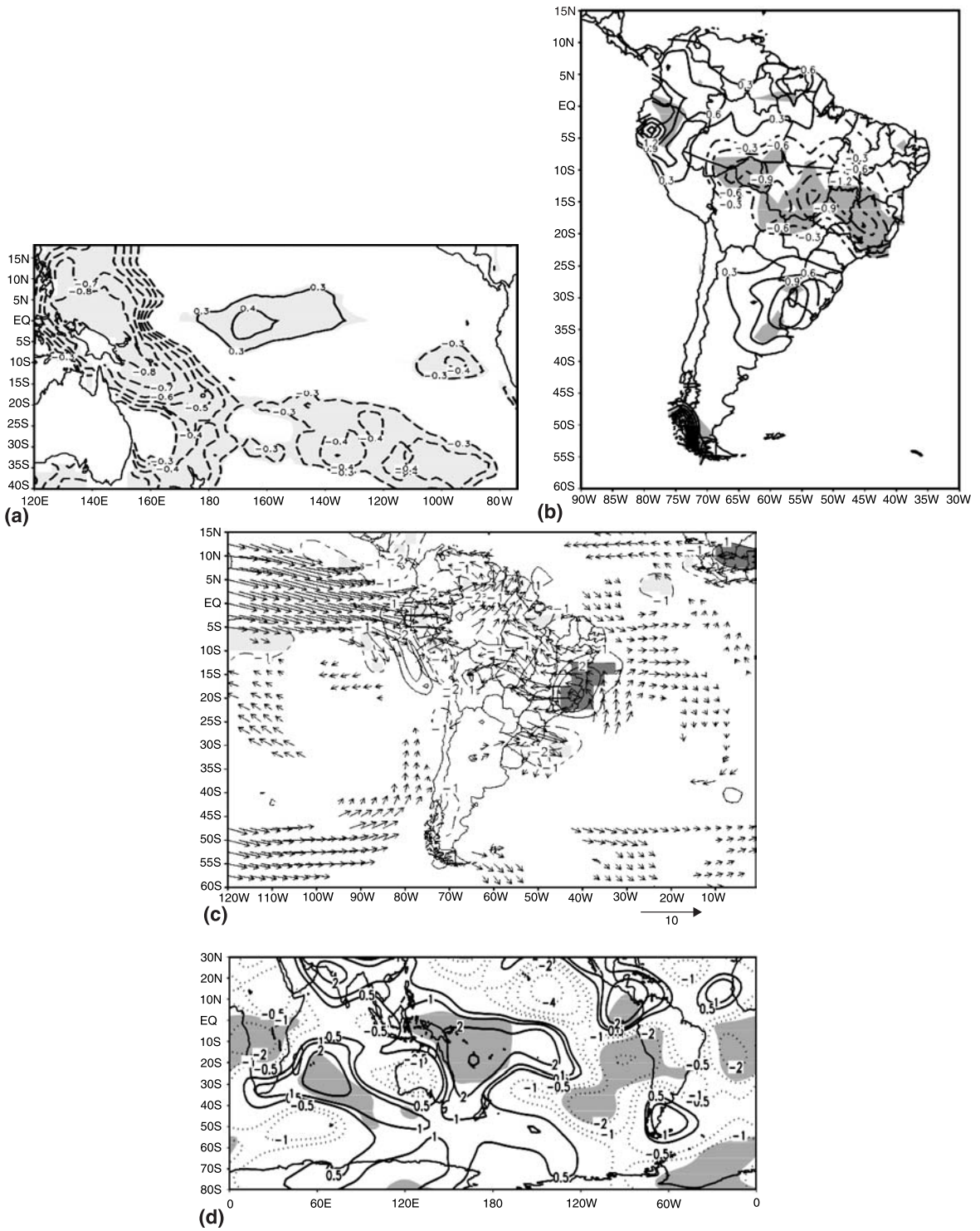

Fig. 3. (**a**–**d**) The same as Fig. 1a–d, but for the second rotated SST variability mode observed in the southern Pacific + Equatorial Pacific Ocean during the austral summer

presents anomalous anticyclonic circulation over southeastern Brazil and anomalous moisture flux divergence over this region, as well as the anomalous northerly moisture flux over the La Plata Basin. However, the model fails in reproducing the anomalous moisture flux convergence over southern Brazil which is presented by the composite in Fig. 3c.

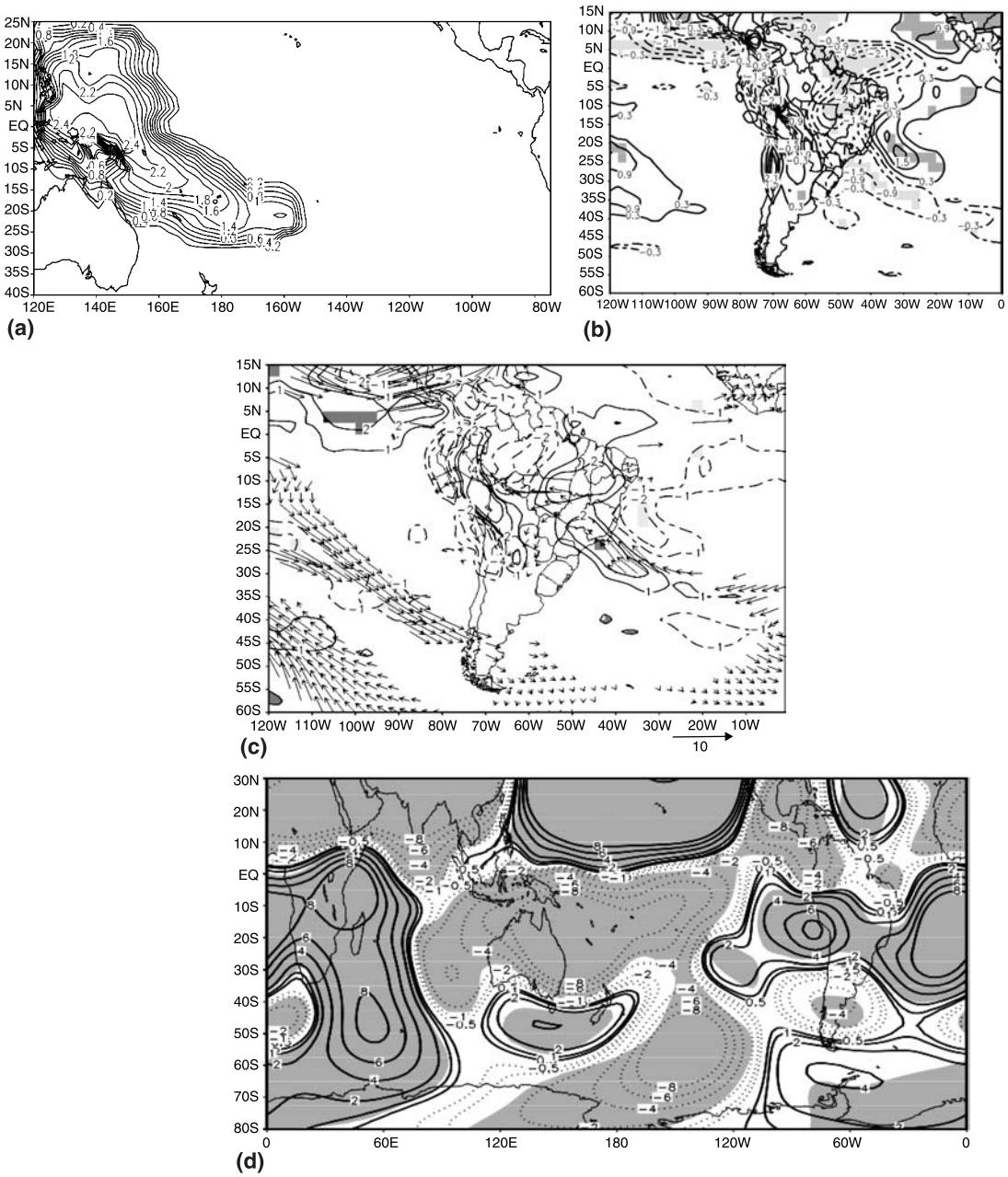

Fig. 4. (**a**–**d**) The same as Fig. 2a–d, but for the second rotated SST variability mode observed in the southern Pacific + Equatorial Pacific Ocean during the austral summer

The upper level circulation indicates a teleconnection pattern similar to that described by Mo (2000), where a wave emanates from the Indonesian region and extends towards South America following an arc-like path (Fig. 4d). Although the model was able to reproduce the wave train emanating from Indonesia, the general pattern is slightly out of phase when compared to the composite map (Fig. 3d). The differences observed between the statistical and numerical results could be explained by the fact that the composite map probably represents the impact of different forcings while the model is forced by a specific one.

3.3 The impact of southwestern South Pacific SST anomalies on South American precipitation during the austral summer

The sixth SEP mode explains 6% of the total variance and is located over the southwestern

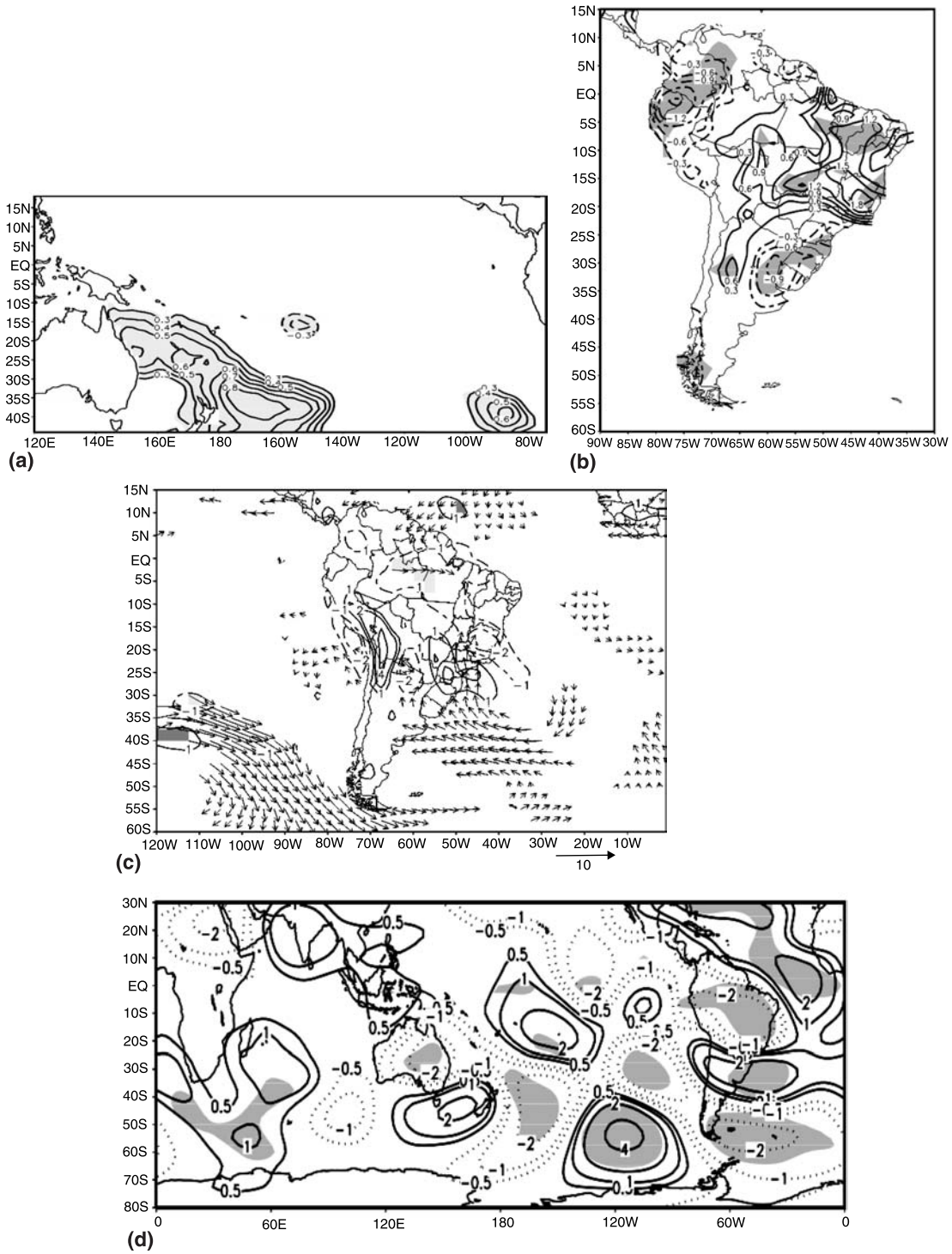

Fig. 5. (**a**–**d**) The same as Fig. 1a–d, but for the sixth rotated SST variability mode observed in the southern Pacific + Equatorial Pacific Ocean during the austral summer

Pacific reaching its maximum value near New Zealand (Fig. 5a). The composites indicate that warmer waters over this region are associated with enhanced precipitation over the SACZ and drought conditions over the sub-tropics (Fig. 5b). The vertically integrated anomalous moisture flux presents anomalous moisture flux convergence over the Amazon Basin and central-eastern Brazil, as well as anomalous cyclonic circulation close to the southeastern Brazil coast, which is

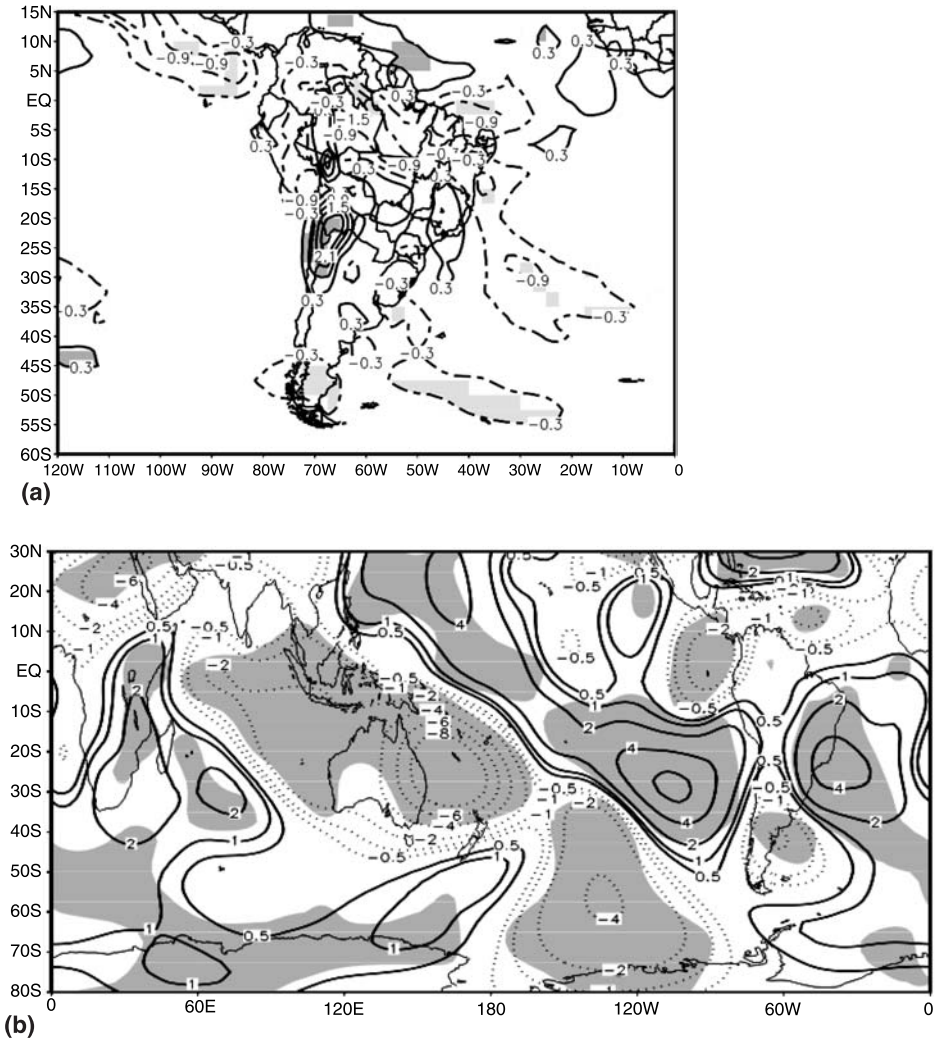

Fig. 6. (**a**) DJF precipitation anomalies (mm day^{-1}) simulated in the experiment forced by the SST anomalies given in the Fig. 5a. Only absolute values higher than 0.3 mm day^{-1} are shown and the interval between the isolines is 0.6 mm day^{-1}; (**b**) the same as **a**, but for the DJF 200 hPa anomalous zonally asymmetric component of stream function ($\times 10^6$ m^2 s^{-1}). The absolute values of the isolines are 0.5; 1; 2; 4; 6×10^6 m^2 s^{-1}

associated with an anomalous southerly moisture flux over southern Brazil (Fig. 5c). The streamfunction anomalous circulation composite suggests the configuration of two anomalous wave trains: one emanating from Indonesia and the other from the central Pacific (Fig. 5d).

Following the procedure used for the other experiments, the GCM was forced by SST anomalies similar to those depicted in Fig. 5a. The model results obtained in this case completely failed to reproduce the atmospheric circulation and South American precipitation patterns obtained from the statistical analysis (Fig. 6). In fact, the wave propagation path and, in particular, the wavenumber were quite different (Fig. 6b). As a consequence, the precipitation pattern observed over the continent (Fig. 6a) does not agree with that shown in Fig. 5b. It seems that besides the forcing imposed in the simulation there are others that may be acting to produce the patterns observed in the analysis. For instance, the wavelength of the waves generated by the model are larger than those observed. This feature could suggest that the interaction between the sub-tropical forcing with the basic state creates a different waveguide in the atmosphere and therefore a different remote response over South America (Ambrizzi and Hoskins 1997, and references therein). On the other hand, some studies have suggested that the impact of regional processes can be as important as remote influences in the modulation of precipitation in some regions (e.g., Grimm 2003). As GCM resolution is usually low, it is very difficult for these models to take into account the variability of some parameters such as soil moisture, topography and others; therefore it could compromise the rainfall simulation. Further experiments related to the SST mode

used here are currently in progress in order to verify why the model was unable to reproduce the observational analysis in this case.

4. Discussion

This work investigates the impact of three different austral summer low-frequency SST variability modes located in the Indian and the Pacific Oceans on the interannual variability of the SAMS using statistical and numerical methodologies. As a statistical analysis cannot explain a dynamic cause by itself, numerical experiments with an atmospheric GCM were conducted in order to study the possible impact of SSTs on the atmosphere.

REOF analysis was applied to the summer SST anomalies observed in the South Pacific + Equatorial Pacific, and in the Indian Oceans in order to obtain the variability modes and the associated extreme events. Numerical simulations using the Community Climate Model version 3.6 (CCM3.6) GCM was carried out. The model was forced with the warm phase of the selected SST modes, which were considered as SST anomalies, through an ensemble technique.

One of the three SST variability modes is located close to southeastern Africa. The statistical results suggest that the warmer waters observed in this region during the austral summer could be related to dry conditions over the SACZ and enhanced precipitation over sub-tropical South America. The numerical results suggest the importance of this forcing on the configuration of the anomalous precipitation patterns observed in the composite maps as the model was able to simulate the positive precipitation anomalies in the sub-tropics and negatives anomalies in the tropics. The simulated atmospheric circulation indicates an austral extra-tropical wave perturbation emanating from the Indian Ocean. This energy activity propagates towards the eastern equatorial Pacific following an arc-like trajectory through the extra-tropics. In fact, this wave trajectory follows the Sub-polar Jet wave guide, a teleconnection pattern originally proposed by Hoskins and Ambrizzi (1993) and Berbery et al. (1992). Saji et al. (2005) have also verified that

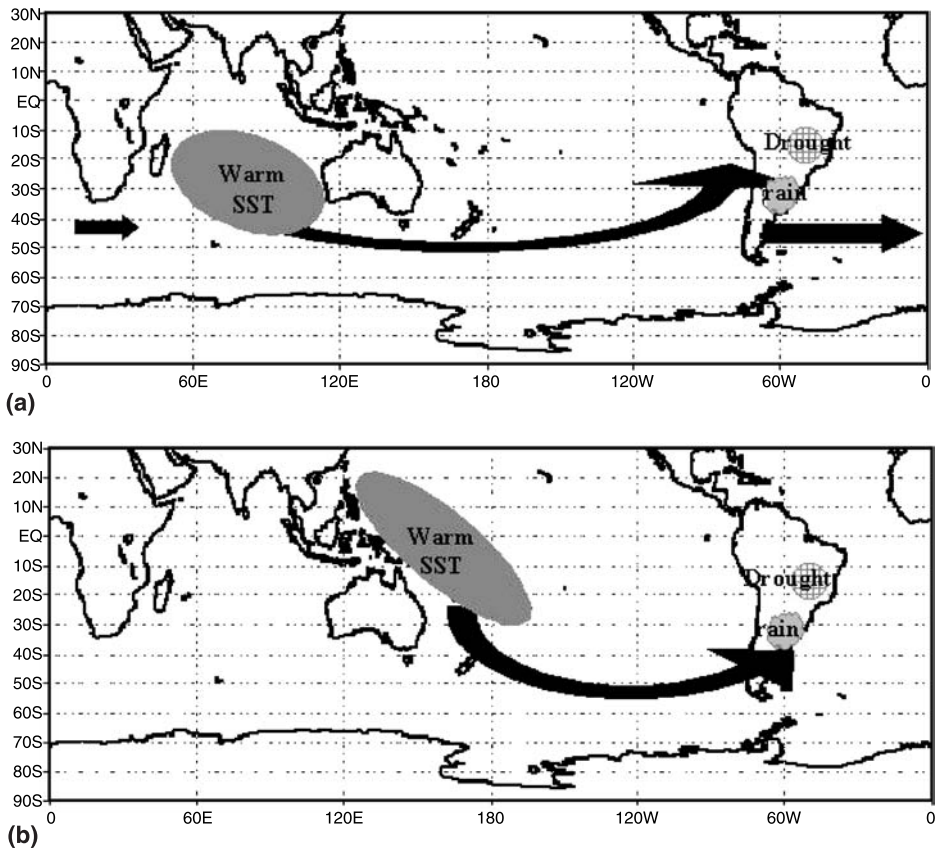

Fig. 7. (**a**) Summary of the impact of the southern Indian Ocean warm SST anomalies over the South American precipitation during the austral summer according to the numerical simulations; (**b**) the same as **a**, but for the western Pacific Ocean warm SST anomalies

the Indian Ocean may have some influence over the South American climate. They found that during the austral spring there is a relationship between the Indian Ocean Dipole and the continental sub-tropical surface air temperature and explain this link through the Rossby wave propagation via the Sub-polar Jet wave guide. Figure 7a summarizes how this forcing impacts South American precipitation according to the numerical simulations.

A second SST variability mode was located in the western Pacific Ocean. Statistical results indicate that warmer waters over Indonesia and the sub-tropical southern Pacific are related to dry conditions over the SACZ and enhanced precipitation over sub-tropical South America. Again, the numerical results indicate that this forcing may affect South American precipitation through the propagation of an anomalous wave train emanating from Indonesia, similar to the PSA 2 pattern of Mo (2000). A schematic summarizing how this forcing may affect South American precipitation according to the numerical simulations is shown in Fig. 7b.

Finally, the third SST variability mode is located over the southwestern South Pacific. According to the statistical results, positive SST anomalies in this region are associated with enhanced precipitation in tropical Brazil and drought in sub-tropical South America during the austral summer. The model was unable to reproduce this pattern. It is suggested that other forcings may be playing an important role in producing the observational pattern, which are not included in the simulation. Further numerical experiments are currently in progress to verify this hypothesis. We must recall that atmospheric GCMs are limited in simulating the air-sea interaction in sub-tropical regions, where the role of the atmosphere on the ocean is important. However, it is first necessary to understand how the ocean can influence the atmosphere in order to utilize coupled models. In this way, coupled GCM simulations could give different answers especially for the sub-tropical forcings.

From the statistical analysis, and some of the numerical experiments shown here, it seems clear that the displacement of the forcing from tropical to sub-tropical regions can have a strong impact on the South American climate. When warmer waters prevail over Indonesia drought conditions are observed over southeastern Brazil. However, the existence of warmer waters over the southwestern Pacific generates normal on higher than average precipitation in the same region. It is interesting to note that the Indian Ocean mode seems to play an important role on the precipitation pattern observed over South America. Further analysis relating this mode with South American rainfall onset during spring is in progress and will be presented elsewhere.

Acknowledgements

We would like to thank the support from Fundação de Amparo à Pesquisa do Estado de São Paulo – FAPESP (proc. 01/06842-6, 01/13816-1, 06/53917-5) and from the Conselho Nacional de Desenvolvimento Científico e Tecnológico – CNPq (proc. 152051/2005-8 and 300348/2005-3). We also wish to thank the Inter America Institute for Global Change Research – IAI (proc. IAI – CRN 055).

References

Ambrizzi T, Hoskins BJ (1997) Stationary Rossby wave propagation in a baroclinic atmosphere. Quart J Roy Meteor Soc 123: 919–928

Ambrizzi T, Souza EB, Pulwarty RS (2004) The Walker and Hadley circulations and associated ENSO impacts on South American seasonal rainfall. In: Diaz HA, Bradley RS (eds) The Hadley circulation: present, past, and future. Kluwer, Dordrecht, pp 203–235

Barros VR, Silvestri GE (2002) The relation between sea surface temperature at the subtropical south-central Pacific and precipitation in southeastern South America. J Climate 15: 251–267

Berbery EH, Paegle JN, Horel JD (1992) Wavelike southern hemisphere extratropical teleconnections. J Atmos Sci 49: 155–177

Casarin DP, Kousky VE (1986) Precipitation anomalies in southern Brazil and atmospheric circulation variations. Rev Bras Meteor 1: 83–90 (in Portuguese)

Chen M, Xie P, Janowiak JE, Arkin PA (2002) Global land precipitation: a 50-yr monthly analysis based on gauge observations. J Hydrometeor 3(3): 249–266

Diaz AF, Studzinski CD, Mechoso CR (1998) Relationship between precipitation anomalies in Uruguay and southern Brazil and sea surface temperature in the Pacific and Atlantic Oceans. J Climate 11: 251–271

Drumond ARM, Ambrizzi T (2005) The role of SST on the South American atmospheric circulation during January, February and March 2001. Clim Dynam 24: 781–791

Figueroa S, Satyamurti P, Silva Dias PL (1995) Simulation of the summer circulation over the South American region with an eta coordinate model. J Atmos Sci 52: 1573–1584

Grimm AM (2003) The El Niño impact on the summer monsoon in Brazil: regional processes versus remote influences. J Climate 16: 263–280

Grimm AM, Ferraz SET, Gomes J (1998) Precipitation anomalies in southern Brazil associated with El Niño and La Niña events. J Climate 11: 2863–2880

Grimm AM, Vera CS, Mechoso CR (2005) The South American monsoon system. In: Chang CP, Wang B, Lau NCG (eds) The global monsoon system: research and forecast. WMO/TD 1266-TMRP70, pp 219–238

Haarsma RJ, Campos EJD, Molteni F (2003) Atmospheric response to South Atlantic SST dipole. Geophys Res Lett 30(16): 1864–1868

Herdies DL, da Silva A, Silva Dias MA, Nieto-Ferreira R (2002) Moisture budget of the bimodal pattern of the summer circulation over South America. J Geophys Res 107: 42/1–42/10

Hoskins BJ, Ambrizzi T (1993) Rossby wave propagation on a realistic longitudinally varying flow. J Atmos Sci 50(12): 1661–1671

Hurrell JW, Hack JJ, Boville BA, Willianson DL, Kiehl JT (1998) The dynamical simulation of the NCAR community climate model version 3. J Climate 11: 1207–1236

Kalnay E, Kanamitsu M, Kistler R, Collins W, Deaven D, Gandin L, Iredell M, Saha S, White G, Woollen J, Zhu Y, Chelliah M, Ebisuzaki W, Higgins W, Janoviak J, Mo KC, Ropelewski C, Wang J, Leetmaa A, Reynolds R, Jenne R, Joseph D (1996) The NCEP/NCAR 40-year reanalysis project. Bull Amer Meteor Soc 77(3): 437–471

Kiehl JT, Hack JJ, Bonan GB, Boville BA, Williamson DL, Rasch PJ (1998) The national center for atmospheric research community climate model: CCM3. J Climate 11: 1131–1149

Kodama YM (1992) Large-scale common features of subtropical precipitation zones (the Baiu frontal zone, SPCZ, and the SACZ): Part I. Characteristics of subtropical frontal zones. J Meteor Soc Japan 70: 813–835

Lenters JD, Cook KH (1995) Simulation and diagnosis of the regional summertime precipitation climatology of South America. J Climate 8: 2988–3005

Liebmann BG, Kiladis GN, Marengo JA, Ambrizzi T, Glick JD (1999) Submonthly convective variability over South America and the South Atlantic Convergence Zone. J Climate 12: 1877–1891

Marengo JA, Douglas M, Silva Dias P (2002) The South American low-level jet east of the Andes during the LBA-TRMM and WET AMC campaign of January–April 1999. J Geophys Res 107: 47/1–47/11

Marengo JA, Soares WR, Saulo C, Nicolini M (2004) Climatology of the low-level Jet east of the Andes as derived from the NCEP reanalyses. J Climate 17: 2261–2280

Mo KC (2000) Relationship between low-frequency variability in the southern hemisphere and sea surface temperature anomalies. J Climate 13: 3599–3610

Nogués-Paegle J, Mo KC (1997) Alternating wet and dry condictions over South America during summer. Mon Wea Rev 125: 279–291

Robertson AW, Mechoso CR (2000) Interannual and interdecadal variability of the South Atlantic convergence zone. Mon Wea Rev 128: 2947–2957

Robertson AW, Farrara JD, Mechoso CR (2003) Simulations of the atmospheric response to South Atlantic sea surface temperature anomalies. J Climate 16: 2540–2551

Ropelewski CF, Halpert MS (1987) Global and regional scale precipitation patterns associated with the El Niño/southern Oscillation. Mon Wea Rev 115: 1606–1626

Saji NH, Ambrizzi T, Ferraz SET (2005) Indian Ocean dipole events and austral surface air temperature anomalies. Dynam Atmos Oceans 39: 87–101

Smith TM, Reynolds RW, Livezey RE, Stokes DC (1996) Reconstruction of historical sea surface temperatures using empirical orthogonal functions. J Climate 9: 1403–1420

Zhou J, Lau KM (2001) Principal modes of interannual and decadal variability of summer rainfall over South America. Int J Climatol 21: 1623–1644